Theory of X-ray grazing incidence reflection in the presence of nuclear resonance excitation

R. Röhlsberger

Fachbereich Physik, Universität Rostock, August-Bebel-Str. 55, D-18055 Rostock, Germany

The dynamical theory of nuclear resonant diffraction is applied to the case of grazing incidence reflection. The solution of the dynamical equations is obtained by evaluation of a matrix exponential. This formalism is applied to grazing incidence reflection from arbitrary stratified media. However, the basic formalism is not restricted to this case, but can be used to describe a wide range of diffraction phenomena. This is demonstrated in the case of grazing incidence diffraction from gratings in the n-beam case. Moreover, the theory is extended to describe the influence of surface and boundary roughness.

1. Introduction

The outstanding brilliance of X-ray synchrotron radiation has opened unique experimental possibilities to study properties of surfaces and thin films. Moreover, the X-ray optical properties of thin films and multilayer systems are often exploited in dispersive elements (filters, monochromators) for synchrotron beamlines. In case of nuclear resonant scattering, it was realized before the first synchrotron-based experiment that thin films can be applied as ultranarrow bandpass filters [1]. The dynamical theory of nuclear resonant X-ray reflection from thin films was then worked out in a series of papers [2,3]. On the basis of this theory, thin film optics has been successfully developed for nuclear resonant filtering of synchrotron radiation [4–6]. During the development of grazing incidence optics it turned out that film systems with a periodicity parallel to the surface normal (multilayers, superlattices) and perpendicular to it (reflection gratings) are promising candidates for the desired kind of filtering as well. It was therefore necessary to extend the dynamical theory of nuclear resonant scattering to include these cases as well [7]. Moreover, the theory should also be able to handle the influence of surface and boundary roughness. In this contribution we will summarize the theory with additional emphasis on multilayer systems and diffraction gratings and the treatment of boundary roughness.

The dynamical theory of nuclear resonant scattering differs from the ordinary dynamical theory of X-ray scattering due to the strong polarization dependence of the scattering amplitude. This polarization dependence arises as soon as the degeneracy of the nuclear levels is lifted by a hyperfine interaction with alignment or texturing of the nuclear moments in the sample. This applies not only for nuclear resonant scattering

at transition energies of Mössbauer nuclei [8] but also for magnetic X-ray scattering in the vicinity of inner-shell resonances [9,10]. The strong polarization dependence enables the determination of magnetic structures, especially when polarization filtering techniques are applied [11]. Moreover, the extremely sharp energy dependence of nuclear resonant scattering allows for novel mechanisms for ultra-high resolution filtering of synchrotron radiation [12–14]. Very similar polarization effects are found in scattering of visible light from magnetic structures, responsible for many kinds of magneto-optical effects [15,16], and in reflection of polarized neutrons from magnetic surfaces [17].

This paper is organized as follows. The first section briefly describes the algebraic structure of the theory, based on the evaluation of an exponential of the scattering matrix. The dimension of the matrix is determined by the scattering geometry and the geometry of the sample. The latter enters through evaluation of the structure function and allows the formalism to be extended to arbitrary sample geometries. In the next section the scattering matrix is derived. It results from the solution of a system of coupled differential equations that describe the propagation of waves in the sample. It turns out that the evaluation of the matrix exponential can be considerably simplified by taking advantage of its symmetry properties, leading to a very intuitive factorization into simple matrices. A separate section is devoted to the treatment of boundary roughness, where a matrix is derived that describes the effect of a continous density transition between two adjacent layers. Finally, the theory is extended to the case of reflection from laterally structured layers, i.e., reflection gratings.

Some remarks about the notation used here: Lower-case boldface letters denote 2×2 matrices, while upper-case boldface letters represent matrices with a dimension $\geqslant 4$. The hat ($\hat{A}$) marks a unit vector, $\vec{A}$ is a 2-component vector, and $\underline{A}$ is a supervector with a dimension $\geqslant 4$. $\mathbf{E}, \mathbf{N}$ and $\mathbf{M}$ are atomic scattering operators that are represented by 2×2 matrices.

2. Algebraic structure of the theory

Basically, every approach to describe the propagation of electromagnetic waves in homogeneous materials leads to a set of coupled linear differential equations with constant coefficients [18]. If converted into a set of first-order equations, such a system can be conveniently solved by calculating the matrix exponential of the coefficient matrix. As a general result, the propagation of electromagnetic waves through a homogeneous medium with thickness d can be described by

$$\underline{\mathrm{A}}(d) = \mathrm{e}^{\mathrm{i}\boldsymbol{F}d}\underline{\mathrm{A}}(0), \tag{2.1}$$

where $\underline{\mathrm{A}}$ denotes a multidimensional vector representing the set of field amplitudes in the open scattering channels. The matrix exponential relates the field amplitudes $\underline{\mathrm{A}}(d)$ at depth d to the incident amplitudes $\underline{\mathrm{A}}(0)$. The number of scattering channels is determined by:

	Type of scattering	Scattering matrix	Scattering channels
A	Forward scattering	$\boldsymbol{F} = \boldsymbol{k}_0 + \boldsymbol{f}$	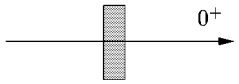
B	Grazing incidence reflection (2-beam diffraction)	$\boldsymbol{F} = \begin{pmatrix} \boldsymbol{f} + \boldsymbol{k}_{0z} & \boldsymbol{f} \\ -\boldsymbol{f} & -\boldsymbol{f} - \boldsymbol{k}_{0z} \end{pmatrix}$	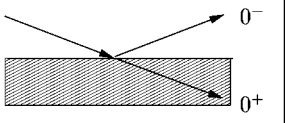
C	N-beam grazing incidence diffraction	$\boldsymbol{F} = \begin{pmatrix} \boldsymbol{k}_{m^+} + \boldsymbol{f}_{m^+m^+} & \cdots & \boldsymbol{f}_{m^+m^-} \\ \vdots & \ddots & \vdots \\ \boldsymbol{f}_{m^-m^+} & \cdots & \boldsymbol{k}_{m^-} + \boldsymbol{f}_{m^-m^-} \end{pmatrix}$	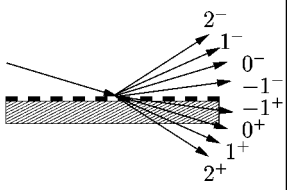

Figure 1. Propagation of electromagnetic waves through homogeneous, anisotropic media of thickness d as described by $\underline{\mathrm{A}}(d) = \mathrm{e}^{\mathrm{i}\boldsymbol{F}d}\underline{\mathrm{A}}(0)$ in case of various scattering geometries. The quantities $\boldsymbol{k}_0$ and $\boldsymbol{f}$ are (2×2) matrices to account for polarization effects. In case of isotropic scattering they reduce to scalars.[1]

(a) The structure of the sample: in crystalline samples, several Bragg- and Laue-reflections are possible. In disordered samples at normal incidence only forward scattering is possible.

(b) The scattering geometry: determines how many scattering channels are actually open, e.g., how many Bragg reflections are simultaneously excited. Regardless of its structure, specular reflection at grazing angles takes place for any sample.

To illustrate this, some examples are listed in figure 1. In case of anisotropic media one has to consider two amplitudes per scattering channel, one for each independent polarization state. The basic features of these cases will be discussed here briefly:

A. *Forward scattering.* This is the most simple case, where only one scattering channel is open. To account for the polarization dependence, $\boldsymbol{F}$ is a 2×2 matrix with

$$\boldsymbol{f} = \begin{pmatrix} f_{xx} & f_{yx} \\ f_{xy} & f_{yy} \end{pmatrix} \quad \text{and} \quad \boldsymbol{k}_0 = \begin{pmatrix} k_0 & 0 \\ 0 & k_0 \end{pmatrix} \tag{2.2}$$

where $\boldsymbol{f}$ is the forward scattering amplitude in an orthogonal polarization basis. The eigenvectors of $\boldsymbol{f}$ represent the eigenpolarizations of the medium. The eigenvalues f_i determine the corresponding refractive indices as defined by $n_i = 1 + f_i/k_0$.

[1] This is only correct in the approximation that the structure function is the same for σ and π polarization, otherwise there is an additional factor of $\gamma = \vec{k}\cdot\vec{k}'/kk' = \cos 2\varphi$ for π polarization. $\boldsymbol{f}$ is then a diagonal (2×2) matrix with $f_{\pi\pi} = \gamma f_{\sigma\sigma}$.

In case of an isotropic medium, eq. (2.1) turns into a scalar equation $A(d) = \mathrm{e}^{\mathrm{i}nk_0 d}\, A(0)$.

B. *Specular reflection.* At grazing angles close to the critical angle, the reflected field cannot be neglected and the two-beam case of dynamical diffraction is encountered. With $\boldsymbol{F}$ a 4×4 matrix, eq. (2.1) describes the polarization amplitudes in two scattering channels: Specular reflection and forward transmission. A detailed derivation of $\boldsymbol{F}$ will be given in the next section.

C. *Diffraction from a reflection grating.* The scattering matrix $\boldsymbol{F}$ contains the scattering matrices for the interaction between all diffraction orders. $\boldsymbol{f}_{m^+n^-}$, for example, describes the amplitude for scattering from the m^+ diffraction order into the n^- diffraction order. A derivation will be given in section 5.

The matrix elements of $\boldsymbol{f}$ are strongly dependent on the scattering geometry, i.e., the orientation of magnetic fields or electric field gradients in the sample relative to the incident wavevector. If the incident polarization does not coincide with one of the eigenpolarizations of the material, orthogonal scattering takes place and there will be a mixing of the eigenpolarizations in the outgoing channel. The strong orientational dependence, combined with the surface sensitivity inherent to grazing incidence X-ray reflection opens a series of applications especially in the study of thin film magnetism [19–21]. As an important example, that is often encountered in the study of magnetic systems, the evaluation of $\boldsymbol{f}$ in case of pure magnetic hyperfine interaction is given in appendix A.

In general, the matrix exponential cannot be calculated analytically. This can be achieved only in a few exceptional cases of 2-beam diffraction. For nuclear Bragg diffraction those are the cases with scattering angles of 180° (backscattering), 90° and 0°. The latter case, which is basically Bragg diffraction with $(hkl) = (000)$, is the main subject of this article. In section 4.4 we will show how the matrix exponential for grazing incidence reflection from anisotropic stratified media can be calculated.

3. Scattering amplitude and structure function

The X-ray scattering response, i.e., the coupling of the scatterer to the incident photons and the amplitude and polarization of the scattered photons are most conveniently described in terms of the scattering operators of the individual atoms. In order to account for the polarization dependence, e.g., in the cases of magnetic X-ray scattering and nuclear resonant scattering, the scattering operators are written as (2×2) matrices in a convenient polarization basis $(\vec{\varepsilon}_a, \vec{\varepsilon}_b)$. Let $\widetilde{\mathbf{M}}(\vec{k}, \omega; \vec{k}', \omega')$ be the total operator for scattering of an incident wave with wavevector $\vec{k}'$ and frequency ω' into a wave with wavevector $\vec{k}$ and frequency ω. The scattered field in first order Born approximation is then given by (momentum representation)

$$\vec{A}_S(\vec{k}, \omega) = -c\, \frac{\delta_+(k, \omega)}{(2\pi)^4} \int \widetilde{\mathbf{M}}(\vec{k}, \omega; \vec{k}', \omega')\, \vec{A}_0(\vec{k}', \omega')\, \mathrm{d}^3k'\, \mathrm{d}\omega' \tag{3.1}$$

with

$$\delta_+(k,\omega) = -\frac{4\pi c}{\omega^2 - k^2c^2 + \mathrm{i}\varepsilon}, \tag{3.2}$$

where $\delta_+(k,\omega)$ is the photon propagator of the outgoing photon. After determination of the scattering operator $\widetilde{\mathbf{M}}(\vec{k},\omega;\vec{k}',\omega')$, the scattered amplitude in real space, $\vec{A}_S(\vec{r},t)$, is obtained from $\vec{A}_S(\vec{k},\omega)$ by Fourier transform.

In the following we will concentrate on elastic scattering, i.e., $\omega' = \omega$. The scattering operator is the sum over the contributions of all atoms in the scattering volume:

$$\widetilde{\mathbf{M}}\big(\vec{k},\omega;\vec{k}',\omega'\big) = \delta\big(\omega'-\omega\big)\sum_j \mathrm{e}^{\mathrm{i}(\vec{k}'-\vec{k})\vec{R}_j}\mathbf{M}_j\big(\vec{k},\omega;\vec{k}',\omega\big). \tag{3.3}$$

$\mathbf{M}_j(\vec{k},\omega;\vec{k}',\omega)$ is the elastic scattering amplitude matrix of the jth atom. Neglecting interference terms between nuclear and electronic scattering, it can be written as the sum of two matrices $\mathbf{E}_j$ and $\mathbf{N}_j$ describing electronic and nuclear scattering, respectively:

$$\mathbf{M}_j\big(\vec{k},\omega;\vec{k}',\omega\big) = \mathbf{E}_j\big(\vec{k},\omega;\vec{k}',\omega\big) + \mathbf{N}_j\big(\vec{k},\omega;\vec{k}',\omega\big). \tag{3.4}$$

Polarization mixing scattering is described by nonvanishing off-diagonal elements of **M**. Explicit expressions for **E** and **N** are given in appendix A. For more details, see [22,23] in the case of nuclear resonant scattering and [9,10] in the case of magnetic X-ray scattering.

Each outgoing wave carries the geometrical phase factor $\mathrm{e}^{\mathrm{i}(\vec{k}'-\vec{k})\vec{R}_j}$ which accounts for the position of the atom in space. We assume that the ensemble of atoms can be divided into subgroups of identical scattering behaviour (e.g., the different components of alloys, the various constituents of crystal lattices), marked by the subscript u. Then the scattering matrix reads

$$\widetilde{\mathbf{M}}\big(\vec{k},\omega;\vec{k}',\omega'\big) = \delta\big(\omega'-\omega\big)\sum_u S_u\big(\vec{k}'-\vec{k}\big)\mathbf{M}_u\big(\vec{k},\omega;\vec{k}',\omega\big). \tag{3.5}$$

All information about the arrangement of the atoms is contained in the structure function $S_u(\vec{q}) = S_u(\vec{k}-\vec{k}')$:

$$S_u\big(\vec{q}\big) = \int_V \rho_u\big(\vec{r}\big)\mathrm{e}^{\mathrm{i}\vec{q}\cdot\vec{r}}\,\mathrm{d}^3r, \tag{3.6}$$

where $\rho_u(\vec{r})$ is the number density of the atoms in subgroup (u). The integration runs over the whole sample volume. In this article we will apply the above formalism to scattering from homogeneous thin films (next section) and laterally structured thin films acting as diffraction gratings (section 5).

4. Scattering from thin films

4.1. Scattering in first order Born approximation

In the following we calculate the scattering response of a thin film in the first order Born approximation. The film is a very thin platelet of thickness b and homogeneous density $\rho_u(\vec{r}) = \rho_u$, extending to infinity in the in-plane directions. The structure function of such a platelet is given by

$$S_u(\vec{q}) = \rho_u \int_{-\infty}^{\infty} \mathrm{d}x\, \mathrm{d}y\, \mathrm{e}^{\mathrm{i}\vec{q}_{xy}\cdot\vec{r}} \int_0^b \mathrm{d}z\, \mathrm{e}^{\mathrm{i}q_z z} = (2\pi)^2 \rho_u \delta^2(\vec{q}_{xy}) \frac{\mathrm{e}^{\mathrm{i}q_z b} - 1}{\mathrm{i}q_z} \tag{4.1}$$

with

$$\vec{q}_{xy} = \vec{k}_{xy} - \vec{k}'_{xy} \quad \text{and} \quad q_z = k_z - k'_z.$$

Assuming the incident wave to be a plane wave, i.e.,

$$\vec{A}_0(\vec{k}', \omega') = (2\pi)^4 \delta(\omega' - \omega_0) \delta^3(\vec{k}' - \vec{k}_0) \vec{A}_0, \tag{4.2}$$

the scattered wave in phase space is obtained explicitly after inserting eq. (3.5) with eq. (4.1) into eq. (3.1):

$$\begin{aligned} \vec{A}_S(\vec{k}, \omega) = &-c(2\pi)^2 \delta_+(k, \omega) \delta(\omega - \omega_0) \delta^2(\vec{q}_{xy}) \frac{\mathrm{e}^{\mathrm{i}q_z b} - 1}{\mathrm{i}q_z} \\ &\times \sum_u \rho_u \mathbf{M}_u(\vec{k}, \omega; \vec{k}_0, \omega_0) \vec{A}_0. \end{aligned} \tag{4.3}$$

The scattered wave in real space is obtained by Fourier transformation of the above expression. The integration over the δ-distributions is easy to perform and the remaining integral over k_z is solved via the residue theorem. The two poles of the photon propagator, eq. (3.2), lead to two solutions for $z > 0$ (below the platelet) and $z < 0$ (above the platelet). These solutions correspond to a transmitted wave in the forward direction, the 0^+ channel, and a reflected wave in the specular direction, the 0^- channel. The wave in the forward direction is given by

$$\vec{A}^{0^+}(\vec{r}, t) = \mathrm{e}^{\mathrm{i}(\vec{k}_{0^+}\cdot\vec{r} - \omega_0 t)} \left(\mathbf{1} + \mathrm{i}b\boldsymbol{f}^{0^+0^+}\right) \vec{A}_0 \tag{4.4}$$

with

$$\boldsymbol{f}^{0^+0^+} = \frac{1}{k_{0^+z}} \sum_u \rho_u \mathbf{M}_u(\vec{k}_{0^+}, \omega_0; \vec{k}_{0^+}, \omega_0)$$

and the wave in the specular direction is given by

$$\vec{A}^{0^-}(\vec{r}, t) = \mathrm{e}^{\mathrm{i}(\vec{k}_{0^-}\cdot\vec{r} - \omega_0 t)} \mathrm{i}b\boldsymbol{f}^{0^-0^+} \vec{A}_0 \tag{4.5}$$

with

$$\boldsymbol{f}^{0^-0^+} = \frac{1}{k_{0^-z}} \frac{\mathrm{e}^{2\mathrm{i}k_{0^-z}b} - 1}{2\mathrm{i}k_{0^-z}b} \sum_u \rho_u \mathbf{M}_u\big(\vec{k}_{0^-}, \omega_0; \vec{k}_{0^+}, \omega_0\big);$$

$\vec{k}_{0^+} = \vec{k}_0$ is the wavevector of the photon field in the 0^+ channel and $\vec{k}_{0^-}$ the wavevector of the photon field in the 0^- channel. The (2×2) matrices $\boldsymbol{f}^{0^+0^+}$ and $\boldsymbol{f}^{0^-0^+}$ describe the scattering from the incident 0^+ channel into the 0^+ and 0^- channels, respectively. **1** is the (2×2) unit matrix.

4.2. Solution of the dynamical scattering equations

For thick layers, especially in grazing incidence geometry, where the scattered field often reaches the magnitude of the incident field, the 1st order Born approximation is no longer valid. This problem is solved by dividing the layer into thin platelets for which the 1st order Born approximation is valid and sum up the contributions of all these platelets.

If we look at three subsequent platelets within the layer, we find the situation which is sketched in figure 2: Three thin plateletes are drawn as horizontal lines numbered with $m-1$, m and $m+1$. They are thin enough for the 1st order Born approximation to be valid for calculation of the scattered waves. Each of the waves incident upon platelet m generates two waves travelling in the 0^+ and 0^- channel. The response to incident $\vec{A}^{0^+}(m)$ is given by eqs. (4.4) and (4.5). The response to incident $\vec{A}^{0^-}(m)$ is obtained by changing 0^+ into 0^- channels and vice versa in eqs. (4.4) and (4.5). Each two contributions in the outgoing channels are added, dropping the phase factor $\mathrm{e}^{\mathrm{i}(\vec{k}_{0xy}\cdot\vec{r}-\omega t)}$:

$$\begin{aligned}
\vec{A}^{0^+}(m+1) &= \mathrm{e}^{\mathrm{i}k_{0^+z}b}\big\{\big(\mathbf{1} + \mathrm{i}b\boldsymbol{f}^{0^+0^+}\big)\vec{A}^{0^+}(m) + \mathrm{i}b\boldsymbol{f}^{0^+0^-}\vec{A}^{0^-}(m)\big\},\\
\vec{A}^{0^-}(m-1) &= \mathrm{e}^{-\mathrm{i}k_{0^-z}b}\big\{\big(\mathbf{1} - \mathrm{i}b\boldsymbol{f}^{0^-0^-}\big)\vec{A}^{0^-}(m) - \mathrm{i}b\boldsymbol{f}^{0^-0^+}\vec{A}^{0^+}(m)\big\}.
\end{aligned} \tag{4.6}$$

In the continuous limit $b \to 0$, i.e., $k_{0z}b \ll 1$, we expand the exponentials, make the substitutions

$$\vec{A}^{0^\pm}(m) \to \vec{A}^{0^\pm}(z), \qquad \vec{A}^{0^\pm}(m \pm 1) \to \vec{A}^{0^\pm}(z \pm b)$$

and expand the last expression around z. Then the system of coupled difference equations converges into a system of coupled differential equations:

$$\begin{aligned}
\frac{\mathrm{d}\vec{A}^{0^+}(z)}{\mathrm{d}z} &= \mathrm{i}\big[\big(\boldsymbol{f}^{0^+0^+} + \boldsymbol{k}\big)\vec{A}^{0^+}(z) + \boldsymbol{f}^{0^+0^-}\vec{A}^{0^-}(z)\big],\\
\frac{\mathrm{d}\vec{A}^{0^-}(z)}{\mathrm{d}z} &= \mathrm{i}\big[\boldsymbol{f}^{0^-0^+}\vec{A}^{0^+}(z) + \big(\boldsymbol{f}^{0^-0^-} - \boldsymbol{k}\big)\vec{A}^{0^-}(z)\big]
\end{aligned} \tag{4.7}$$

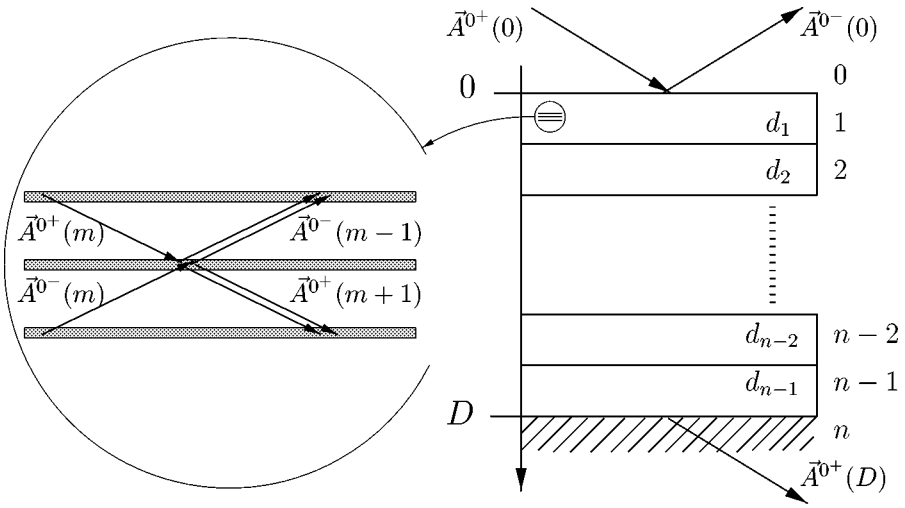

Figure 2. Wavefields in the dynamical theory of X-ray diffraction (left) and scheme of a layer system (right). The task is to solve for the field amplitudes $\vec{A}^{0-}(0)$ and $\vec{A}^{0+}(D)$ under the boundary conditions $\vec{A}^{0+}(0) = \vec{A}_0$ and $\vec{A}^{0-}(D) = 0$.

with $\boldsymbol{k} = k_{0z}\mathbf{1}$. By combining $\vec{A}^{0+}(z)$ and $\vec{A}^{0-}(z)$ into one supervector $\underline{\mathrm{A}}$, these equations can be written in matrix style:

$$\frac{\mathrm{d}\underline{\mathrm{A}}(z)}{\mathrm{d}z} = \mathrm{i}\boldsymbol{F}\underline{\mathrm{A}}(z) \tag{4.8}$$

with

$$\boldsymbol{F} = \begin{pmatrix} \boldsymbol{f}^{0^+0^+} + \boldsymbol{k} & \boldsymbol{f}^{0^+0^-} \\ \boldsymbol{f}^{0^-0^+} & \boldsymbol{f}^{0^-0^-} - \boldsymbol{k} \end{pmatrix} \quad \text{and} \quad \underline{\mathrm{A}}(z) = \begin{pmatrix} \vec{A}^{0+}(z) \\ \vec{A}^{0-}(z) \end{pmatrix}.$$

If the scattering matrix $\boldsymbol{F}$ is independent of z, this equation has the immediate solution

$$\underline{\mathrm{A}}(z) = \mathrm{e}^{\mathrm{i}\boldsymbol{F}z}\underline{\mathrm{A}}(0). \tag{4.9}$$

This equation relates the field amplitudes at depth z to the field amplitudes on the surface of the layer. The solution eq. (4.9) is only complete if it is supplemented by the boundary conditions

$$\vec{A}^{0+}(0) = \vec{A}_0 \quad \text{and} \quad \vec{A}^{0-}(D) = 0. \tag{4.10}$$

At the surface the only field propagating in the 0^+ direction is the incident wave $\vec{A}_0$. At the opposite boundary we assume for the moment that there is no wave traveling in the 0^- direction. This implies that we have a free-standing layer that is not supported by a substrate. It will be shown later how a semi-infinite substrate is introduced.

4.3. Calculation of field amplitudes

In order to solve for either the specularly reflected field $\vec{A}^{0^-}(0)$ or the transmitted field $\vec{A}^{0^+}(D)$, eq. (4.9) has to be evaluated for $z = D$. Equation (4.9) is now rewritten by expressing the vectors $\vec{A}(0)$ and $\vec{A}(D)$ explicitly in their 0^+ and 0^- components, decomposing the matrix $e^{i\boldsymbol{F}D}$ into (2×2) submatrices $\boldsymbol{s}_{++}$, $\boldsymbol{s}_{+-}$, $\boldsymbol{s}_{-+}$ and $\boldsymbol{s}_{--}$ and inserting the boundary conditions:

$$\begin{pmatrix} \vec{A}^{0^+}(D) \\ 0 \end{pmatrix} = \begin{pmatrix} \boldsymbol{s}_{++} & \boldsymbol{s}_{+-} \\ \boldsymbol{s}_{-+} & \boldsymbol{s}_{--} \end{pmatrix} \begin{pmatrix} \vec{A}_0 \\ \vec{A}^{0^-}(0) \end{pmatrix}. \tag{4.11}$$

This equation can now be solved for the reflected and transmitted field amplitude as well as for the amplitude at any depth inside the layer system:

(a) *The reflected amplitude.* Solving eq. (4.11) for the specularly reflected field $\vec{A}^{0^-}(0)$, we obtain

$$\vec{A}^{0^-}(0) = -[\boldsymbol{s}_{--}]^{-1}\boldsymbol{s}_{-+}\vec{A}_0. \tag{4.12}$$

(b) *The transmitted amplitude.* With the solution for $\vec{A}^{0^-}(0)$ it is now possible to solve for the transmitted field $\vec{A}^{0^+}(D)$:

$$\vec{A}^{0^+}(D) = \boldsymbol{s}_{++} - \boldsymbol{s}_{+-}[\boldsymbol{s}_{--}]^{-1}\boldsymbol{s}_{-+}\vec{A}_0. \tag{4.13}$$

(c) *The amplitude at depth z.* Once the reflected amplitude $\vec{A}^{0^-}(0)$ is known, the amplitude at any depth z can be calculated:

$$\vec{A}^{0^+}(z) = \boldsymbol{s}_{++}(z) - \boldsymbol{s}_{+-}(D)\big[\boldsymbol{s}_{--}(D)\big]^{-1}\boldsymbol{s}_{-+}(z)\vec{A}_0. \tag{4.14}$$

This is applied, for example, to estimate the fluorescence yield from thin films [24–26] or the performance of X-ray waveguide structures [27,28].

The above procedure is basically independent of the shape of $\boldsymbol{F}$. We will show in section 5 how it is applied in case of diffraction gratings.

If the scattering matrix $\boldsymbol{F}$ is a function of depth, the layer is subdivided into thin slices within which $\boldsymbol{F}$ is constant. The problem is then solved by calculating the matrix product of all the individual layer matrices. This procedure will be outlined in section 4.5.

From the computational point of view, the treatment is already complete at this point. However, further simplifications that make use of the special symmetry of the scattering matrix in grazing incidence geometry lead to a clearer representation as well as a numerically more efficient algorithm, as will be shown in the following section.

4.4. Evaluation of the layer matrix exponential

The matrix exponential is easily calculated after diagonalization of $\boldsymbol{F}$. In grazing incidence geometry this can be done analytically because the matrices $\boldsymbol{f}^{ss'}$ $(s, s' =$

$0^+, 0^-$) can be expressed to a very good approximation by the forward scattering matrix $\boldsymbol{f}^{0^+0^+}$ and therefore can be diagonalized simultaneously:

$$\boldsymbol{f} = \boldsymbol{f}^{0^+0^+} = \boldsymbol{f}^{0^+0^-} = -\boldsymbol{f}^{0^-0^+} = -\boldsymbol{f}^{0^-0^-} =: \begin{pmatrix} f_{xx} & f_{xy} \\ f_{yx} & f_{yy} \end{pmatrix}, \tag{4.15}$$

where $\boldsymbol{f}^{0^+0^+}$ is given explicitly by eq. (4.4). Now $\boldsymbol{F}$ reads

$$\boldsymbol{F} = \begin{pmatrix} \boldsymbol{f} + \boldsymbol{k} & \boldsymbol{f} \\ -\boldsymbol{f} & -\boldsymbol{f} - \boldsymbol{k} \end{pmatrix}. \tag{4.16}$$

The diagonalization of this matrix is not only a formal procedure. Quite interestingly, the result is a factorization into matrices with a very intuitive physical interpretation.

$\boldsymbol{F}$ is diagonalized in two steps: First, the (2×2) forward scattering matrix $\boldsymbol{f}$ is diagonalized, i.e.,

$$\boldsymbol{f} = \boldsymbol{g}\, \boldsymbol{f}_e\, \boldsymbol{g}^{-1} \quad \text{with} \quad \boldsymbol{g} = \begin{pmatrix} 1 & 1 \\ \dfrac{f_1 - f_{xx}}{f_{xy}} & \dfrac{f_2 - f_{xx}}{f_{xy}} \end{pmatrix} \tag{4.17}$$

and

$$f_{1,2} = \frac{1}{2}(f_{xx} + f_{yy}) \pm \frac{1}{2}\sqrt{(f_{xx} - f_{yy})^2 + 4 f_{xy} f_{yx}}\,, \tag{4.18}$$

where f_1, f_2 are the eigenvalues of $\boldsymbol{f}$. The matrix $\boldsymbol{g}$ consists of the eigenvectors of $\boldsymbol{f}$, which are the eigenpolarizations of the material. The eigenpolarizations are those polarization states that remain unchanged while traveling through the material. Now $\boldsymbol{F}$ can be rewritten as the following matrix product:

$$\boldsymbol{F} = \boldsymbol{G}\boldsymbol{F}_e\boldsymbol{G}^{-1} = \begin{pmatrix} \boldsymbol{g} & \boldsymbol{0} \\ \boldsymbol{0} & \boldsymbol{g} \end{pmatrix} \begin{pmatrix} (\boldsymbol{f}_e + \boldsymbol{k}) & \boldsymbol{f}_e \\ -\boldsymbol{f}_e & -(\boldsymbol{f}_e + \boldsymbol{k}) \end{pmatrix} \begin{pmatrix} \boldsymbol{g}^{-1} & \boldsymbol{0} \\ \boldsymbol{0} & \boldsymbol{g}^{-1} \end{pmatrix}. \tag{4.19}$$

The matrix $\boldsymbol{F}_e$ is the representation of $\boldsymbol{F}$ in the basis of eigenpolarizations. Note that $\boldsymbol{F}_e$ is in a simple blockdiagonal shape and can therefore be written as the direct product of two submatrices representing both eigenpolarizations. This is just the expression of the fact that the eigenpolarizations in a medium travel independently of each other. Thus, the diagonalization of $\boldsymbol{F}_e$ can be reduced to two independent problems, each for every eigenpolarization. As a result, $\boldsymbol{F}_e$ can be written as the following product of matrices:

$$\boldsymbol{F}_e = \begin{pmatrix} \boldsymbol{t}_{01}^{-1} & \boldsymbol{0} \\ \boldsymbol{0} & \boldsymbol{t}_{01}^{-1} \end{pmatrix} \begin{pmatrix} \boldsymbol{1} & \boldsymbol{r}_{01} \\ \boldsymbol{r}_{01} & \boldsymbol{1} \end{pmatrix} \begin{pmatrix} \boldsymbol{q}_1 & \boldsymbol{0} \\ \boldsymbol{0} & -\boldsymbol{q}_1 \end{pmatrix} \begin{pmatrix} \boldsymbol{1} & \boldsymbol{r}_{10} \\ \boldsymbol{r}_{10} & \boldsymbol{1} \end{pmatrix} \begin{pmatrix} \boldsymbol{t}_{10}^{-1} & \boldsymbol{0} \\ \boldsymbol{0} & \boldsymbol{t}_{10}^{-1} \end{pmatrix} \tag{4.20}$$

with

$$\boldsymbol{r}_{01} = \begin{pmatrix} r_{01,1} & 0 \\ 0 & r_{01,2} \end{pmatrix}, \quad \boldsymbol{t}_{01} = \begin{pmatrix} t_{01,1} & 0 \\ 0 & t_{01,2} \end{pmatrix}, \quad \text{and} \quad \boldsymbol{q}_1 = \begin{pmatrix} k_{0z}\beta_{1,1} & 0 \\ 0 & k_{0z}\beta_{1,2} \end{pmatrix},$$

where $r_{01,i}$ and $t_{01,i}$ are the Fresnel reflection and transmission coefficients for both eigenpolarizations, labeled by $i = 1, 2$, at the boundary between vacuum and the material:

$$r_{01,i} = \frac{1-\beta_{1,i}}{1+\beta_{1,i}}, \qquad t_{01,i} = \frac{2}{1+\beta_{1,i}}. \tag{4.21}$$

The coefficients $\beta_{1,i}$ relate the z-component of the wavevector in the material to the wavevector of the incident wave:

$$k_{1z,i} = k_{0z}\beta_{1,i} \quad \text{with} \quad \beta_{1,i} = \sqrt{1 + \frac{2f_i}{k_{0z}}}, \quad i = 1, 2. \tag{4.22}$$

Putting eqs. (4.19) and (4.20) together we finally express the layer matrix exponential $\boldsymbol{S}$ as the following matrix product:

$$\boldsymbol{S} = \mathrm{e}^{\mathrm{i}\boldsymbol{F}d} = \boldsymbol{G}_1\boldsymbol{T}_{01}^{-1}\boldsymbol{R}_{01}\boldsymbol{E}_1\boldsymbol{R}_{10}\boldsymbol{T}_{10}^{-1}\boldsymbol{G}_1^{-1}. \tag{4.23}$$

Each matrix appearing here has an obvious physical interpretation:

$\boldsymbol{G}_1 = \begin{pmatrix} \boldsymbol{g}_1 & \boldsymbol{0} \\ \boldsymbol{0} & \boldsymbol{g}_1 \end{pmatrix}$ is the transformation matrix that mediates the transition from the basis of eigenpolarizations to the orthogonal polarization basis chosen for representation.

$\boldsymbol{T}_{01} = \begin{pmatrix} \boldsymbol{t}_{01} & \boldsymbol{0} \\ \boldsymbol{0} & \boldsymbol{t}_{01} \end{pmatrix}$ describes the transmission of both eigenpolarizations through the interface between vacuum and layer 1.

$\boldsymbol{R}_{01} = \begin{pmatrix} \boldsymbol{1} & \boldsymbol{r}_{01} \\ \boldsymbol{r}_{01} & \boldsymbol{1} \end{pmatrix}$ describes the reflection of both eigenpolarizations at the interface between vacuum and layer 1.

$\boldsymbol{E}_1 = \begin{pmatrix} \mathrm{e}^{\mathrm{i}\boldsymbol{q}_1 d} & \boldsymbol{0} \\ \boldsymbol{0} & \mathrm{e}^{-\mathrm{i}\boldsymbol{q}_1 d} \end{pmatrix}$ describes the propagation of the two eigenpolarizations through the layer. In the dynamical theory the wavefield in the medium is the superposition of two waves propagating in positive and negative z directions.

4.5. Scattering from multiple layers

This formalism is easily extended to the general case of multiple layers. Assume a layer system consisting of n layers with the scattering matrices F_i, thicknesses d_i,

and total thickness $D = \sum_{i=1}^{n} d_i$. Then the field in the nth layer, i.e., at depth $z > d_s = \sum_{i=1}^{n-1} d_i$, is given by

$$\vec{A}(z) = \mathrm{e}^{\mathrm{i}\boldsymbol{F}_n(z-d_s)}\mathrm{e}^{\mathrm{i}\boldsymbol{F}_{n-1}d_{n-1}} \cdots \mathrm{e}^{\mathrm{i}\boldsymbol{F}_2 d_2}\mathrm{e}^{\mathrm{i}\boldsymbol{F}_1 d_1}\vec{A}(0). \tag{4.24}$$

For convenience we introduce the following matrix:

$$\boldsymbol{S} = \mathrm{e}^{\mathrm{i}\boldsymbol{F}_n d_n}\mathrm{e}^{\mathrm{i}\boldsymbol{F}_{n-1}d_{n-1}} \cdots \mathrm{e}^{\mathrm{i}\boldsymbol{F}_2 d_2}\mathrm{e}^{\mathrm{i}\boldsymbol{F}_1 d_1}. \tag{4.25}$$

With the matrices introduced above, the layer matrix exponential for a two-layer sandwich can be written as

$$\boldsymbol{S} = \boldsymbol{S}_2\boldsymbol{S}_1 = \boldsymbol{G}_2\boldsymbol{T}_{02}^{-1}\boldsymbol{R}_{02}\boldsymbol{E}_2\boldsymbol{R}_{21}\boldsymbol{E}_1\boldsymbol{R}_{10}\boldsymbol{T}_{10}^{-1}\boldsymbol{G}_1^{-1}, \tag{4.26}$$

where we have introduced the interface matrix $\boldsymbol{R}_{21}$:

$$\boldsymbol{R}_{21} = \boldsymbol{T}_{20}^{-1}\boldsymbol{R}_{20}\boldsymbol{G}_{21}\boldsymbol{R}_{01}\boldsymbol{T}_{01}^{-1} \quad \text{with} \quad \boldsymbol{G}_{21} = \boldsymbol{G}_2^{-1}\boldsymbol{G}_1. \tag{4.27}$$

The concept of the interface matrix allows us to write the product of matrix exponentials for an n-layer system in a convenient way:

$$\boldsymbol{S} = \boldsymbol{R}_{n,n-1}\prod_{k=n-1}^{1}\boldsymbol{E}_k\boldsymbol{R}_{k,k-1}, \tag{4.28}$$

where $\boldsymbol{R}_{ij}$ is given by

$$\boldsymbol{R}_{ij} = \begin{pmatrix} \boldsymbol{a}_{ij} & \boldsymbol{b}_{ij} \\ \boldsymbol{b}_{ij} & \boldsymbol{a}_{ij} \end{pmatrix} \quad \text{with} \quad \begin{aligned} \boldsymbol{a}_{ij} &= \boldsymbol{t}_{i0}^{-1}(\boldsymbol{g}_{ij} + \boldsymbol{r}_{i0}\boldsymbol{g}_{ij}\boldsymbol{r}_{0j})\boldsymbol{t}_{0j}^{-1}, \\ \boldsymbol{b}_{ij} &= \boldsymbol{t}_{i0}^{-1}(\boldsymbol{r}_{i0}\boldsymbol{g}_{ij} + \boldsymbol{g}_{ij}\boldsymbol{r}_{0j})\boldsymbol{t}_{0j}^{-1}. \end{aligned} \tag{4.29}$$

Here, we have already assumed that the layer system is supported by a substrate, i.e., layer n with infinite thickness. In evaluating eq. (4.25) we have carried out the limit $\lim_{d\to\infty}\mathrm{e}^{\mathrm{i}\boldsymbol{g}d} = \boldsymbol{0}$. This is just the expression of the fact that in a semi-infinite medium the waves traveling in the 0^+ direction vanish with increasing depth.

This is the general result for an arbitrary layer system where, for example, the magnetization direction varies from layer to layer. This is observed, e.g., in case of magnetic twist grain boundaries, where the magnetization rotates from one direction into another across a layer boundary.

The above formalism can be further simplified if the eigenpolarizations of all layers are the same. In this case $\boldsymbol{G}_{21} = \boldsymbol{1}$, and the interface matrix $\boldsymbol{R}_{21}$ simplifies to[2]

$$\boldsymbol{R}_{21} = \boldsymbol{T}_{20}^{-1}\boldsymbol{R}_{20}\boldsymbol{R}_{01}\boldsymbol{T}_{01}^{-1} = \begin{pmatrix} \boldsymbol{t}_{21}^{-1} & \boldsymbol{0} \\ \boldsymbol{0} & \boldsymbol{t}_{21}^{-1} \end{pmatrix}\begin{pmatrix} \boldsymbol{1} & \boldsymbol{r}_{21} \\ \boldsymbol{r}_{21} & \boldsymbol{1} \end{pmatrix}. \tag{4.30}$$

[2] In deriving eq. (4.30) we have used the following relations between the Fresnel coefficients: $t_{ij} = t_{i0}t_{0j}/(1 + r_{i0}r_{0j})$ and $r_{ij} = (r_{i0} + r_{0j})/(1 + r_{i0}r_{0j})$.

The problem can now be solved for each eigenpolarization separately. We apply eq. (4.28) for a single coating on a semi-infinite substrate:

$$\boldsymbol{S} = \boldsymbol{R}_{21}\boldsymbol{E}_1\boldsymbol{R}_{10} \tag{4.31}$$

and we obtain the classical thin-film multibeam interference formula [29]

$$r_{012} = \frac{r_{01} + r_{12}\mathrm{e}^{2\mathrm{i}k_{0z}\beta_1 d_1}}{1 + r_{01}r_{12}\mathrm{e}^{2\mathrm{i}k_{0z}\beta_1 d_1}}. \tag{4.32}$$

This equation can be used to calculate the reflectivity of a stack of layers recursively by inserting r_{012} instead of r_{12} when adding the next layer on top. Since, in general, the eigenpolarizations of the layer system do not coincide with the polarization basis chosen, a transformation back into that basis has to be performed. The (2×2) reflectivity matrix as defined through eq. (4.12) is then given by

$$\boldsymbol{r} = \boldsymbol{g}\boldsymbol{r}_{\mathrm{e}}\boldsymbol{g}^{-1} \tag{4.33}$$

with $[\boldsymbol{r}_{\mathrm{e}}]_{ij} = \delta_{ij}R_i$. Here, the R_i are the reflectivities of the layer system for both eigenpolarizations, according to eq. (4.32). Evaluation of eq. (4.33) then leads to the following closed expression for $\boldsymbol{r}$:

$$\boldsymbol{r} = \begin{pmatrix} \frac{1}{2}\left(R_+ + R_-\left(\frac{f_{xx}-f_{yy}}{f_1-f_2}\right)\right) & R_-\left(\frac{f_{xy}}{f_1-f_2}\right) \\ R_-\left(\frac{f_{yx}}{f_1-f_2}\right) & \frac{1}{2}\left(R_+ - R_-\left(\frac{f_{xx}-f_{yy}}{f_1-f_2}\right)\right) \end{pmatrix} \tag{4.34}$$

with $R_\pm = R_1 \pm R_2$.

4.6. Treatment of surface roughness

In the preceding section the matrix exponential $\mathrm{e}^{\mathrm{i}\boldsymbol{F}z}$ was evaluated in order to calculate the field of a wave at depth z of a material characterized by the scattering matrix $\boldsymbol{F}$. The calculation of the field in layered media is accomplished by multiplication of the corresponding matrix exponentials. This procedure is only valid for layers of homogeneous density, i.e., where $\boldsymbol{F}$ is independent of z. However, in the case of boundary roughness we encounter a situation where the density may vary continuously over a certain range. Then the above formalism can be applied again if the layer system is subdivided into thin slices of homogeneous density. A drawback is the increase in computational effort which accompanies such a procedure. Therefore a closed solution is attempted which replaces the effect of the transition region by one single "roughness matrix" $\mathrm{e}^{\boldsymbol{W}}$. The transition from the case of a smooth boundary to a rough boundary shall be accomplished by inserting this matrix $\mathrm{e}^{\boldsymbol{W}}$ between the two exponential matrices of the adjacent layers:

$$\mathrm{e}^{\mathrm{i}\boldsymbol{F}_2 d_2}\mathrm{e}^{\mathrm{i}\boldsymbol{F}_1 d_1} \longrightarrow \mathrm{e}^{\mathrm{i}\boldsymbol{F}_2 d_2}\mathrm{e}^{\boldsymbol{W}}\mathrm{e}^{\mathrm{i}\boldsymbol{F}_1 d_1}; \tag{4.35}$$

$\boldsymbol{W}$ is expected to be a function of the scattering matrices $\boldsymbol{F}_1$, $\boldsymbol{F}_2$ and σ is a parameter characterizing the thickness of the transition region.

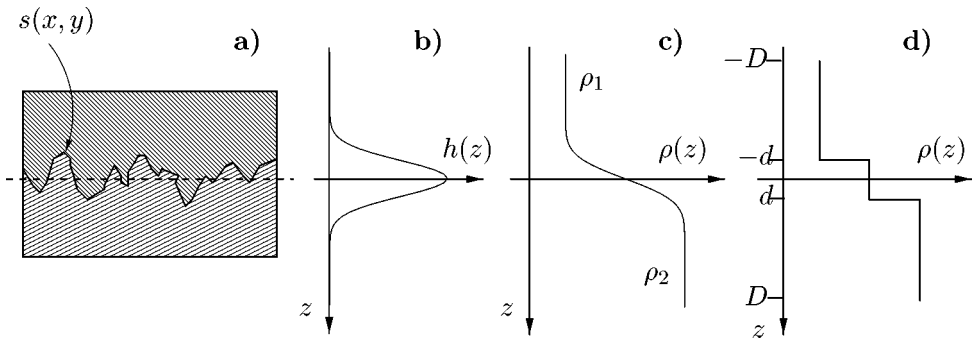

Figure 3. Density variation around a rough interface between two layers with densities ρ_1 and ρ_2. (a) Rough boundary between two materials with densities ρ_1 and ρ_2. $s(x, y)$ is the surface profile function. (b) Height distribution function $h(z)$ describes the probability to find an element of the surface at depth z. (c) Density transition $\rho(z)$ as obtained from integration over the height distribution function. (d) Simplified model of (c), leading to eq. (4.36).

In a simple model, let us first assume that the rough boundary is represented by a transition layer with thickness $2d$, centered around the common boundary between two layers of thickness D each, see figure 3. The scattering matrices of these layers are given by $\boldsymbol{F}_1$ and $\boldsymbol{F}_2$, respectively, the scattering matrix of the transition region is $(\boldsymbol{F}_1 + \boldsymbol{F}_2)/2$. With the above ansatz, the product of the exponential matrices is then given by

$$\begin{aligned} \mathrm{e}^{\mathrm{i}\boldsymbol{F}_2 D}\mathrm{e}^{\boldsymbol{W}}\mathrm{e}^{\mathrm{i}\boldsymbol{F}_1 D} &= \mathrm{e}^{\mathrm{i}\boldsymbol{F}_2 D}\,\mathrm{e}^{-\mathrm{i}\boldsymbol{F}_2 d}\,\mathrm{e}^{\mathrm{i}(\boldsymbol{F}_1+\boldsymbol{F}_2)d}\,\mathrm{e}^{-\mathrm{i}\boldsymbol{F}_1 d}\,\mathrm{e}^{\mathrm{i}\boldsymbol{F}_1 D} \\ &= \mathrm{e}^{\mathrm{i}\boldsymbol{F}_2 D}\,\mathrm{e}^{-(1/2)\mathrm{i}[\boldsymbol{F}_2,\boldsymbol{F}_1]d}\,\mathrm{e}^{\mathrm{i}\boldsymbol{F}_1 D}, \end{aligned} \tag{4.36}$$

where we have made use of the Campbell–Baker–Hausdorff (CBH) relation:

$$\mathrm{e}^{\boldsymbol{A}}\mathrm{e}^{\boldsymbol{B}} = \mathrm{e}^{\boldsymbol{A}+\boldsymbol{B}+(1/2)[\boldsymbol{A},\boldsymbol{B}]}; \tag{4.37}$$

$[\boldsymbol{A}, \boldsymbol{B}] = \boldsymbol{AB} - \boldsymbol{BA}$ is the commutator between $\boldsymbol{A}$ and $\boldsymbol{B}$. Commutators of higher than second order have been neglected, which is reasonable if the thickness of the transition region is small. Moreover, in this approximation every matrix exponential with second order exponents commutes with matrices of first order exponents. As a result, the matrix $\boldsymbol{W}$ we are looking for is expected to contain commutators of various orders between $\boldsymbol{F}_1$ and $\boldsymbol{F}_2$.

Now we want to develop a more realistic model of the transition region. In any case, however, we concentrate only on the specular reflection. Fluctuations of the optical properties perpendicular to the surface normal lead to diffuse scattering. A corresponding theory for X-ray diffuse scattering including polarization effects has just been developed on the basis of the distorted-wave Born approximation [30]. This, however, is beyond the scope of this paper. Here, it is assumed that the roughness can be treated as a continuous density transition along the surface normal. In grazing incidence geometry this assumption is justified as long as only the specularly reflected radiation is considered and the condition $k_z\sigma \ll 1$ holds. In the following the rough

boundary is located around $z = 0$, surrounded by two layers with densities ρ_1 and ρ_2 and equal thickness $d \gg \sigma$, see figure 3.

The boundary plane is defined as the average smooth surface for which $\int s(x, y)\,\mathrm{d}x\,\mathrm{d}y = 0$ holds, where $s(x, y)$ is the surface profile function, measured relative to that plane. For derivation of the roughness matrix we subdivide the density transition region into thin slices of constant density and multiply the layer matrices of all these layers. An outline of the computational procedure is given in the appendix. The result is

$$\boldsymbol{W} = \frac{1}{2}[\boldsymbol{F}_1, \boldsymbol{F}_2] \int_{-\infty}^{\infty} z^2 h(z)\,\mathrm{d}z + \frac{1}{24}\big[\big[[\boldsymbol{F}_1, \boldsymbol{F}_2], \boldsymbol{F}_1\big], \boldsymbol{F}_2\big] \int_{-\infty}^{\infty} z^4 h(z) dz + \cdots$$

$$= \sum_{n=1}^{\infty} \frac{\langle h(z)\rangle_{2n}}{(2n)!} [\boldsymbol{F}_1, \boldsymbol{F}_2]_{2n}, \tag{4.38}$$

where $\langle h(z)\rangle_{2n}$ is the $(2n)$th moment of the height distribution function $h(z)$ and $[\boldsymbol{F}_1, \boldsymbol{F}_2]_{2n}$ is the commutator of order $2n$ between $\boldsymbol{F}_1$ and $\boldsymbol{F}_2$, i.e., $[\boldsymbol{F}_1, \boldsymbol{F}_2]_2 = [\boldsymbol{F}_1, \boldsymbol{F}_2]$, $[\boldsymbol{F}_1, \boldsymbol{F}_2]_4 = [[[\boldsymbol{F}_1, \boldsymbol{F}_2], \boldsymbol{F}_1], \boldsymbol{F}_2]$, and so on.

This is the general result for taking into account roughness described by a density transition which follows from a height distribution. In this limit it is valid for all kinds of scattering phenomena that are described in the exponential matrix formalism, especially grazing incidence diffraction with polarization mixing and diffraction from laterally structured surfaces.

In the special case of a Gaussian height distribution we have

$$h(z) = \frac{1}{\sqrt{2\pi}\sigma}\,\mathrm{e}^{-z^2/(2\sigma^2)} \quad \text{and} \quad \big\langle h(z)\big\rangle_{2n} = (2n-1)!!\sigma^{2n}, \tag{4.39}$$

so that the roughness matrix is given by

$$\boldsymbol{W} = \sum_{n=1}^{\infty} \frac{1}{n!}\left(\frac{\sigma^2}{2}\right)^n [\boldsymbol{F}_1, \boldsymbol{F}_2]_{2n}. \tag{4.40}$$

A closed expression for this series has so far been found only in the special case that the eigenpolarizations for all layers are the same. In appendix B it will be shown that the above result leads to the widely accepted formula for the treatment of surface roughness obtained by Nevot and Croce [31].

5. Grazing incidence diffraction from reflection gratings

Reflection gratings are widely used as monochromatizing elements in spectrometers for energies from the infrared to the range of soft X-rays. They are just becoming interesting also for hard X-rays with respect to the analysis of microstructures [32,33], and they are conceptually new in the field of nuclear resonant scattering. By producing gratings with an isotopic or magnetic superstructure, pure nuclear reflections can be

created that can be used for ultra-narrow monochromatization of synchrotron radiation. A detailed example will be discussed in [34].

Diffraction from a reflection grating relies on the interference between waves reflected from different parts of the surface. Interference only takes place if the incoming wavefield has a sufficiently large degree of transverse coherence. In this section we present the formalism of the dynamical theory of X-ray diffraction for the case of reflection from a planar grating. The treatment is an extension of the formalism described in the preceding section.

Of special interest in the experiments described here is the diffraction from rectangular gratings because of the unique phase shift occurring between different parts of the incoming beam upon reflection. The geometry is shown in figure 4. In analogy to the treatment in the preceding section, this grating is assumed to be very thin so that the 1st order Born approximation is valid. The structure function is given by

$$S(\vec{q}) = \rho \sum_{n=-\infty}^{\infty} \int_{na-(d/2)}^{na+(d/2)} \mathrm{d}x\, \mathrm{e}^{\mathrm{i}q_x x} \int_{-\infty}^{\infty} \mathrm{d}y\, \mathrm{e}^{\mathrm{i}q_y y} \int_0^b \mathrm{d}z\, \mathrm{e}^{\mathrm{i}q_z z}. \tag{5.1}$$

After carrying out the sum and performing the integrations we obtain

$$S(\vec{q}) = -(2\pi)^2 \frac{\rho}{a} \frac{(\mathrm{e}^{\mathrm{i}q_x d} - 1)(\mathrm{e}^{\mathrm{i}q_z b} - 1)\mathrm{e}^{-\mathrm{i}q_x d/2}}{q_x q_z} \delta(q_y) \sum_{m=-\infty}^{\infty} \delta\left(q_x - \frac{2\pi m}{a}\right). \tag{5.2}$$

Each summand corresponds to a certain diffraction order. The further treatment proceeds in the same way as in the case of grazing incidence reflection. We assume a very thin layer of thickness b and treat each diffraction order separately, which results in a solution above and below the scattering plane, respectively. The diffraction orders below the scattering plane, observed in transmission, are labeled by a plus sign, the orders above the scattering plane, the reflected orders, are marked by a minus sign.

The z-component of the wavevector of the wave in the mth diffraction order is given by

$$k_{m^{\pm}z} = \pm\sqrt{k_{0z}^2 - mg(2k_{0x} + mg)}, \tag{5.3}$$

where $g = 2\pi/a$ is the reciprocal lattice unit vector of the grating. Equation (5.3) allows one to determine the range of open scattering channels, i.e., possible diffraction

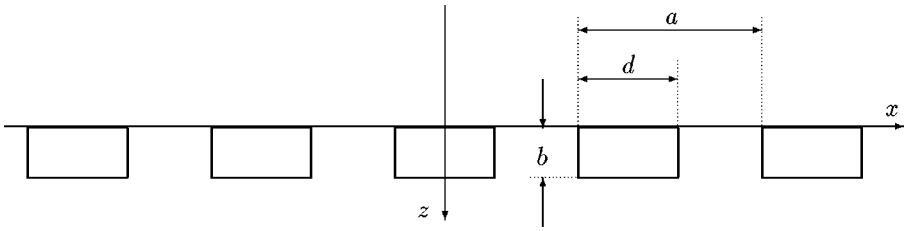

Figure 4. Geometry of a rectangular grating (cross-section).

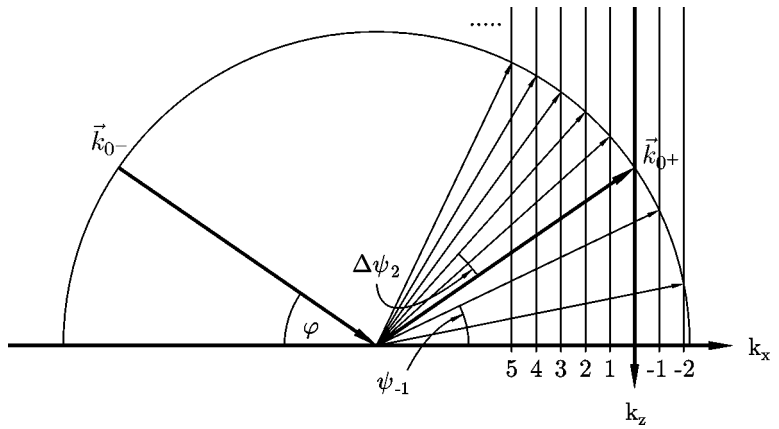

Figure 5. Diffraction at a reflection grating. In reciprocal space a grating is represented by parallel sheets. The intersection points with the Ewald circle indicate the direction of the diffraction orders.

orders. Open channels are those for which $k_{m^{\pm}z}$ is a real quantity. The boundaries of this interval, i.e., the maximum and minimum diffraction order, are given by $m_{\min} \approx -\mathrm{INT}(a\varphi^2/2\lambda)$ and $m_{\max} \approx \mathrm{INT}(2a/\lambda)$, where INT means the integer function. Figure 5 illustrates the different appearance of positive and negative diffraction orders. Below a certain angle of incidence, no negative diffraction orders are observed. The number of positive diffraction orders can be very large, since it scales directly with the ratio of the lattice spacing a to the wavelength λ. All open channels form a closed set, i.e., the waves coming from diffraction at the pth plane, incident upon the $(p+1)$th plane, generate waves which fall into the same set of diffraction orders. The above treatment yields the following expression for the scattering amplitude for scattering from the m^+ channel into the n^+ channel:

$$\begin{aligned} \boldsymbol{f}^{m^+n^+} &= \boldsymbol{f}^{m^+n^-} = -\boldsymbol{f}^{m^-n^+} = -\boldsymbol{f}^{m^-n^-} \\ &= \frac{\rho}{k_{m^+z}} \frac{\sin(\pi(m-n)q)}{\pi(m-n)} \mathbf{M}\big(\vec{k}_0, \omega_0; \vec{k}_0, \omega_0\big). \end{aligned} \tag{5.4}$$

The resulting total amplitude in the m^+ diffraction order is the result of contributions from all other diffraction orders scattering into this particular order. Summing all these contributions, one finally obtains the following system of coupled differential equations:

$$\begin{aligned} \frac{\mathrm{d}\vec{A}^{m^+}(z)}{\mathrm{d}z} &= \mathrm{i} \sum_n \big[\big(\boldsymbol{f}^{m^+n^+} + \delta_{m^+n^+}\boldsymbol{k}_{m^+z}\big)\vec{A}^{n^+}(z) + \boldsymbol{f}^{m^+n^-}\vec{A}^{n^-}(z)\big], \\ \frac{\mathrm{d}\vec{A}^{m^-}(z)}{\mathrm{d}z} &= \mathrm{i} \sum_n \big[\boldsymbol{f}^{m^-n^+}\vec{A}^{n^+}(z) + \big(\boldsymbol{f}^{m^-n^-} + \delta_{m^-n^-}\boldsymbol{k}_{m^-z}\big)\vec{A}^{n^-}(z)\big]. \end{aligned} \tag{5.5}$$

By combining all the vectors $\vec{A}^{m^{\pm}}$ into one supervector, this system of equations can again be written in matrix style and solved by a matrix exponential:

$$\frac{\mathrm{d}\underline{A}(z)}{\mathrm{d}z} = \mathrm{i}\boldsymbol{F}\underline{A}(0) \quad \Longrightarrow \quad \underline{A}(z) = \mathrm{e}^{\mathrm{i}\boldsymbol{F}z}\underline{A}(0) =: \begin{pmatrix} \boldsymbol{S}_{++} & \boldsymbol{S}_{+-} \\ \boldsymbol{S}_{-+} & \boldsymbol{S}_{--} \end{pmatrix} \underline{A}(0). \tag{5.6}$$

This solution is valid if the matrix $\boldsymbol{F}$ is independent of z, which is the case for a rectangular grating. The dimension of $\boldsymbol{F}$ is $4(m_{\max} - m_{\min} + 1)$ with polarization dependence taken into account. As shown above, this can be a considerably large number, which cannot be handled on ordinary computers. However, in many cases a satisfactory accuracy can already be achieved by confining the calculation to a small number N of diffraction orders. In the following the amplitudes in the transmitted and reflected diffraction orders are calculated for a grating of thickness L on a reflecting surface. The boundary conditions specify the values of $\underline{A}^{+}(0)$ and $\underline{A}^{-}(L)$:

$$\begin{aligned} \left[\underline{A}^{+}(0)\right]_m &= \delta_{0m}\vec{A}_0, \\ \left[\underline{A}^{-}(L)\right]_m &= \boldsymbol{r}_{02}(\psi_m)\left[\underline{A}^{+}(L)\right]_m. \end{aligned} \tag{5.7}$$

$\boldsymbol{r}_{02}(\psi_m)$ is the (2×2) reflectivity matrix of the substrate for radiation incident at the diffraction angle ψ_m of the mth diffraction order. By proceeding in a similar way as in the transition from eq. (4.11) to eq. (4.12) we obtain the field amplitude in the mth reflected diffraction order:

$$\begin{aligned} &\vec{A}^{m^{-}}(0) = \boldsymbol{r}_m \vec{A}_0 \quad \text{with} \\ &\boldsymbol{r}_m = -\boldsymbol{P}_{m^{-}}(\boldsymbol{S}_{--} - \boldsymbol{R}_{02}\boldsymbol{S}_{+-})^{-1}(\boldsymbol{S}_{-+} - \boldsymbol{R}_{02}\boldsymbol{S}_{++})\boldsymbol{P}_{0^{+}}. \end{aligned} \tag{5.8}$$

$\boldsymbol{P}_{m^{-}}$ and $\boldsymbol{P}_{0^{+}}$ are projection matrices, whose combined action in the above equation is to project out the (2×2) submatrix which describes the scattering from the incident 0^{+} channel into the outgoing m^{-} channel. A significant simplification of the calculations can be achieved by taking into account the symmetry of $\boldsymbol{F}$ [7].

This treatment represents the dynamical theory for diffraction from rectangular gratings. Gratings of any other shape can be composed of thin rectangular gratings, where the corresponding exponential matrices have to be multiplied consecutively.

6. Summary

The dynamical theory of X-ray diffraction has been outlined for the case of anisotropic scattering. This occurs, for example, in magnetic materials, especially in the vicinity of inner-shell and nuclear resonances. The latter case is given special emphasis here, even though the formalism is valid for both; the main differences are in the evaluation of the scattering amplitude. The theory presented is based on the calculation of the matrix exponential of the scattering matrix, the matrix elements of which represent the "transition amplitudes" between the scattering channels. In the special case of grazing incidence diffraction, the transitions between the scattering

channels can be described to a very good approximation in terms of the (2×2) matrix of the forward scattering amplitude. This leads to an analytic solution that is not possible in the general case of anisotropic 2-beam Bragg diffraction. Closed expressions were derived for the reflectivity of a general multilayer system. The treatment of a rough boundary as a multilayer system with a continuous density transition yielded a single roughness matrix representing that boundary. It could be shown that for common eigenpolarizations of all layers the result is practically identical to the formula of Nevot and Croce for X-ray reflection from rough interfaces.

The algebraic structure of the theory allows an easy extension to the general case of n-beam diffraction. This was demonstrated in case of diffraction from planar gratings illuminated in grazing incidence geometry. An interesting application would be the extension of the theory to anisotropic grazing incidence diffraction, where a surface Bragg reflection is excited under total reflection conditions. This may allow new experiments in the field of surface magnetism.

The numerical evaluation of the layer-matrix exponential can be performed very efficiently by taking advantage of the special symmetry of the layer matrix. The theory presented here has been implemented in a computer program to be used with the CONUSS distribution [23] and is available from the author.[3] Another, very efficient algorithm has been developed by Deák et al. [35] that is described in this collection [36].

Acknowledgement

It is a pleasure for me to acknowledge stimulating discussions with J.P. Hannon and S.K. Sinha.

Appendix A. Evaluation of the forward scattering amplitude

The electronic elastic forward scattering amplitude $\mathbf{E}_j(\vec{k},\omega;\vec{k}',\omega)$ is diagonal:

$$\left[\mathbf{E}\left(\vec{k},\omega;\vec{k},\omega\right)\right]_{\mu\nu} = 2\pi\delta_{\mu\nu}\left[-r_0\left(F_{\mathrm{e}}(0)+\Delta F_{\mathrm{a}}\right)+\mathrm{i}\frac{k}{4\pi}\sigma_t(\omega)\right], \tag{A.1}$$

where $F_{\mathrm{e}}(0)$ is the atomic form factor, which, for forward scattering at X-ray energies, is equal to Z, the atomic number. ΔF_{a} is the correction to the form factor due to anomalous scattering, which becomes significant near absorption edges. $\sigma_t(\omega)$ is the total absorption cross-section at the photon energy $\hbar\omega$.

The nuclear forward scattering amplitude for an LM multipole oscillator in case of a pure magnetic hyperfine interaction is given by

$$\left[\mathbf{N}\left(\vec{k}_0,\omega;\vec{k}_0,\omega\right)\right]_{\mu\nu} = \sum_{M=-L}^{L}\left[\hat{e}^*_\mu\cdot\widehat{Y}_{LM}\left(\vec{k}_0\right)\right]\left[\widehat{Y}^*_{LM}\left(\vec{k}_0\right)\cdot\hat{e}_\nu\right]F_{LM}(\omega), \tag{A.2}$$

[3] Present e-mail address: roehle@physik1.uni-rostock.de.

which describes the scattering of an incident wave with wavevector $\vec{k}_0$ and polarization $\hat{e}_\nu$ into an outgoing wave with wavevector $\vec{k}_0$ and polarization $\hat{e}_\mu$. The vector spherical harmonics $\widehat{Y}_{LM}(\hat{k})$ describe the emission characteristics of the oscillator. The representation of these functions is given in a spherical polar coordinate frame that is aligned along the quantization axis, which is given here by the direction of the magnetic field $\widehat{B}$.

The energy dependence of the scattering amplitude is contained in the F_{LM}, which are a linear combination of single resonances belonging to each value of M, weighted with the Clebsch–Gordan coefficients, which account for the angular momentum coupling:

$$F_{LM}(\omega) = \frac{4\pi\lambda f_{MB}}{2j_0+1}\frac{1}{1+\alpha}\sum_{m_0=-j_0}^{j_0}\frac{C(j_0\,L\,j_1;m_0\,M)^2}{x(m_0\,M)-i} \tag{A.3}$$

with $x(m_0\,M) = 2[E(j_1;m_0+M) - E(j_0;m_0) - \hbar\omega]/\Gamma$ being the deviation of the energy from the unsplit resonance energy, measured in units of the natural linewidth Γ_0. The sum runs over all ground-state levels.

The vector spherical harmonics for an M1 transition as in the case of the 14.4 keV resonance of ^{57}Fe are given by

$$\widehat{Y}_{10} = \mathrm{i}\sqrt{\frac{3}{8\pi}}\sin\theta\hat{e}_\phi, \qquad \widehat{Y}_{11} = \widehat{Y}^*_{1-1} = \sqrt{\frac{3}{16\pi}}\,\mathrm{e}^{\mathrm{i}\phi}\left[\hat{e}_\theta + \mathrm{i}\cos\theta\hat{e}_\phi\right]. \tag{A.4}$$

$\widehat{Y}_{10}$ describes a linear polarization, while $\widehat{Y}_{11}$ and $\widehat{Y}_{1-1}$ describe left- or right-handed polarization, respectively. $\hat{e}_\theta$ und $\hat{e}_\phi$ are the polar unit vectors. The choice of the wavevector $\vec{k}_0$ of the incident radiation $\vec{k}$ as quantization axis has the advantage that relative phase factors between magnetic sublattices are calculated in a unique way. With the above definitions it is now possible to evaluate the elements of the forward scattering matrix $\hat{f}$ according to eq. (A.2). After some algebra (expressing trigonometric functions by the scalar products $\hat{k}_0\cdot\widehat{B}$, $\hat{\sigma}\cdot\widehat{B}$ and $\hat{\pi}\cdot\widehat{B}$) we finally obtain:

$$\boldsymbol{f} = \frac{3}{16\pi}\begin{pmatrix} F_1+F_{-1} & -\mathrm{i}(\hat{k}_0\cdot\widehat{B})(F_1-F_{-1}) \\ \quad +(\hat{\pi}\cdot\widehat{B})^2(2F_0-F_1-F_{-1}) & \quad -(\hat{\sigma}\cdot\widehat{B})(\hat{\pi}\cdot\widehat{B})(2F_0-F_1-F_{-1}) \\ \mathrm{i}(\hat{k}_0\cdot\widehat{B})(F_1-F_{-1}) & F_1+F_{-1} \\ \quad -(\hat{\sigma}\cdot\widehat{B})(\hat{\pi}\cdot\widehat{B})(2F_0-F_1-F_{-1}) & \quad +(\hat{\sigma}\cdot\widehat{B})^2(2F_0-F_1-F_{-1}) \end{pmatrix}. \tag{A.5}$$

This expression allows us to discuss various scattering geometries in a convenient way. Of special interest are often the cases where $\boldsymbol{f}$ is diagonal in a linear polarization basis. They can be summarized as follows:

- Special orientations of $\hat{k}_0$ relative to $\widehat{B}$: $\widehat{B} \parallel \hat{\sigma}$ and $\widehat{B} \parallel \hat{\pi}$.

- Special distributions of magnetic orientations as in 2D and 3D polycrystallinity. The scattering matrix for these cases is easily obtained by integration over the corresponding orientational distribution of magnetic fields. Some of these cases have been discussed in detail in [37].
- No hyperfine interaction at all. In this case there is a single, unsplit resonance and the scattering is isotropic.

Appendix B. Derivation of the roughness matrix

Here, we give an outline of the derivation of the roughness matrix in eq. (4.38). It is assumed that the roughness can be translated into a continuous density transition. The density variation across the boundary is described by a transition function $u(z) \in [0,1]$ with $\lim_{z\to-\infty} u(z) = 0$ and $\lim_{z\to\infty} u(z) = 1$.[4] Then the density at depth z is given by

$$\rho(z) = \rho_1 - (\rho_1 - \rho_2)u(z). \tag{B.1}$$

Since the scattering amplitude matrix $\boldsymbol{f}$ is proportional to the density ρ of the material, the z-dependence of the scattering matrix $\boldsymbol{F}(z)$ can be written as

$$\boldsymbol{F}(z) = \begin{cases} \boldsymbol{F}_1 - \boldsymbol{F}_{12}u(z), & z < 0, \\ \boldsymbol{F}_2 + \boldsymbol{F}_{12}v(z), & z > 0, \end{cases} \tag{B.2}$$

with $\boldsymbol{F}_{12} = \boldsymbol{F}_1 - \boldsymbol{F}_2$ and $v(z) = 1 - u(z)$. We divide each layer into n slices of homogeneous density and infinitesimal thickness $\delta = d/n$. For abbreviation we set $u_m := u(-m\delta)$ and $v_m := v(m\delta)$ and substitute $\mathrm{i}\delta\boldsymbol{F}_{1,2,12} \to \boldsymbol{F}_{1,2,12}$. Then the field at $z = d$ is related to the field at $z = -d$ by $\vec{A}(d) = \boldsymbol{S}_n\vec{A}(-d)$ with the matrix $\boldsymbol{S}_n$ given by

$$\boldsymbol{S}_n = \underbrace{\mathrm{e}^{\boldsymbol{F}_2+\boldsymbol{F}_{12}v_n}\cdots\mathrm{e}^{\boldsymbol{F}_2+\boldsymbol{F}_{12}v_2}\mathrm{e}^{\boldsymbol{F}_2+\boldsymbol{F}_{12}v_1}}\,\underbrace{\mathrm{e}^{\boldsymbol{F}_1-\boldsymbol{F}_{12}u_1}\mathrm{e}^{\boldsymbol{F}_1-\boldsymbol{F}_{12}u_2}\cdots\mathrm{e}^{\boldsymbol{F}_1-\boldsymbol{F}_{12}u_n}}. \tag{B.3}$$

The underbracing groups the layers above and below the average boundary at $z = 0$. The central problem here is to evaluate these matrix products. In the approximation made here, we apply the CBH equation (eq. (4.37)) to second order, i.e., we assume that the matrices $\boldsymbol{F}_1$ and $\boldsymbol{F}_2$ commute with their commutator. We multiply the matrices in each group successively in the order of increasing index i, thereby making use of the following relations which can easily be proven by induction:

$$\begin{aligned} \mathrm{e}^{\boldsymbol{F}_1-\boldsymbol{F}_{12}u_n}\mathrm{e}^{n\boldsymbol{F}_1} &= \mathrm{e}^{(n+1)\boldsymbol{F}_1}\mathrm{e}^{-\boldsymbol{F}_{12}u_n}\mathrm{e}^{(n+1/2)[\boldsymbol{F}_1,\boldsymbol{F}_{12}]u_n}, \\ \mathrm{e}^{n\boldsymbol{F}_2}\mathrm{e}^{\boldsymbol{F}_2+\boldsymbol{F}_{12}v_n} &= \mathrm{e}^{(n+1/2)[\boldsymbol{F}_2,\boldsymbol{F}_{12}]v_n}\mathrm{e}^{\boldsymbol{F}_{12}v_n}\mathrm{e}^{(n+1)\boldsymbol{F}_2}. \end{aligned} \tag{B.4}$$

[4] The function $u(z)$ can be derived from the height distribution function $h(z)$, which gives the probability of finding an element of the boundary at coordinate z: $u(z) = \int_{-\infty}^{z} h(\varepsilon)\,\mathrm{d}\varepsilon$.

The result is, after the resubstitutions $\boldsymbol{F}_{1,2,12} \rightarrow \mathrm{i}\delta\boldsymbol{F}_{1,2,12}$:

$$\boldsymbol{S}_n = \mathrm{e}^{\mathrm{i}\boldsymbol{F}_1 d}\mathrm{e}^{\boldsymbol{W}_n}\mathrm{e}^{\mathrm{i}\boldsymbol{F}_2 d} \quad \text{with}$$
$$\boldsymbol{W}_n = \sum_{k=1}^{n}\left(k-\frac{1}{2}\right)[\boldsymbol{F}_1,\boldsymbol{F}_2](u_k+v_k) + \boldsymbol{F}_{12}(v_k-u_k). \tag{B.5}$$

In the limit $n \rightarrow \infty$ the sums convert into integrals, where $kd/n \equiv z$ is the spatial coordinate, $\delta = d/n \equiv \mathrm{d}z$ and $u_k \equiv u(z)$, $v_k \equiv v(z) = 1 - u(z)$. Integrations with $u(z)$ and $v(z)$ involved have to be integrated over $[0,-d]$ and $[0,d]$, respectively. If the thickness of the density transition region is small compared to the film thickness d, the error introduced by extending the integration intervals to $[0,-\infty]$ and $[0,\infty]$, respectively, is negligible. In this "continuum" limit the matrix $\boldsymbol{W}_n$ becomes:

$$\boldsymbol{W} = -[\boldsymbol{F}_1,\boldsymbol{F}_2]\left(\int_{-\infty}^{0} z u(z)\,\mathrm{d}z + \int_{0}^{\infty} z v(z)\,\mathrm{d}z\right)$$
$$+ \mathrm{i}\boldsymbol{F}_{12}\left(\int_{-\infty}^{0} u(z)\,\mathrm{d}z + \int_{0}^{\infty} v(z)\,\mathrm{d}z\right). \tag{B.6}$$

This lenghty expression can be simplified considerably. We integrate by parts, observing that $\mathrm{d}u(z)/\mathrm{d}z = h(z)$. The rightmost expression in brackets turns out to be the first moment of $h(z)$, which is zero by definition. The remaining integrals turn out to give the second moment of the height distribution function, so that we finally obtain

$$\boldsymbol{W} = \frac{1}{2}[\boldsymbol{F}_1,\boldsymbol{F}_2]\int_{-\infty}^{\infty} z^2 h(z)\,\mathrm{d}z. \tag{B.7}$$

The higher order terms of eq. (4.38) result from a treatment where the CBH equation is applied to higher orders.

Appendix C. Roughness matrix for isotropic media

Here, we show that in case of equal eigenpolarizations for the adjacent layers, the roughness matrix in eq. (4.40) merges into the result obtained by Nevot and Croce [31], i.e., the reflection coefficient of a rough boundary is affected according to $r_{ij} \rightarrow r_{ij}\mathrm{e}^{-2k_{0z}\beta_i\beta_j\sigma^2}$.

Under these conditions the matrices $\boldsymbol{f}_1$ and $\boldsymbol{f}_2$ commute, the problem can be solved for each eigenpolarization separately, and a closed expression for the $(2n)$th order commutator can be derived:

$$[\boldsymbol{F}_1,\boldsymbol{F}_2]_{2n} = \begin{pmatrix} \boldsymbol{0} & \boldsymbol{b}_n \\ \boldsymbol{b}_n & \boldsymbol{0} \end{pmatrix} \quad \text{with } b_n = k_{0z}^2\left(\beta_2^2-\beta_1^2\right)\left(2k_{0z}^2\right)^{n-1}\left(\beta_1^2+\beta_2^2\right)^{n-1}, \tag{C.1}$$

where we have expressed the f_i by the β_i according to eq. (4.22). Since all matrices appearing in the above equation are diagonal, the problem can be solved for

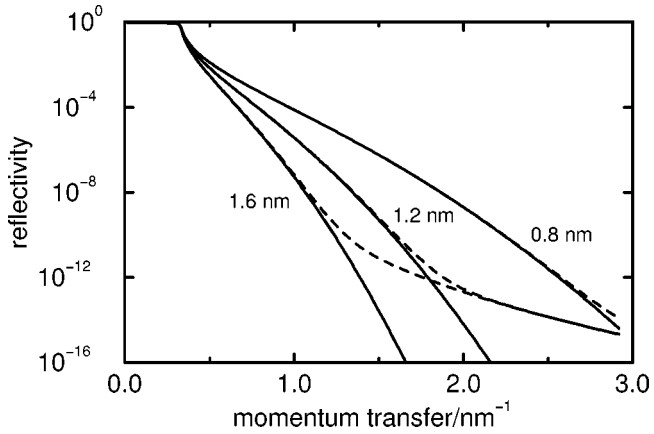

Figure 6. The reflectivity of a Pd boundary for different roughness values, calculated according to the formula of Nevot and Croce [31] (solid lines) and the roughness matrix developed here (dashed lines).

each eigenpolarization separately. Based on the above expression, the summation in eq. (4.40) can be carried out exactly and one obtains for $\boldsymbol{W}$

$$\boldsymbol{W} = \begin{pmatrix} 0 & c \\ c & 0 \end{pmatrix} \quad \text{with } c = \frac{1}{2}\frac{\beta_1^2 - \beta_2^2}{\beta_1^2 + \beta_2^2}\left(1 - \exp\left\{-k_{0z}^2\left(\beta_2^2 + \beta_1^2\right)\sigma^2\right\}\right). \tag{C.2}$$

After evaluation of the roughness matrix $\mathrm{e}^{\boldsymbol{W}}$ the interface matrix $\boldsymbol{R}_{21}$ can be calculated according to eq. (4.27). In case of identical eigenpolarizations of the adjacent layers we have $\boldsymbol{G}_{21} = \mathbf{1}$. After some algebra[5] we finally obtain the interface matrix of the rough boundary:

$$\boldsymbol{R}_{21} = \begin{pmatrix} 1 & \beta_2^{-1} \\ 1 & -\beta_2^{-1} \end{pmatrix} \begin{pmatrix} \mathrm{e}^{c} & 0 \\ 0 & \mathrm{e}^{-c} \end{pmatrix} \begin{pmatrix} 1 & 1 \\ \beta_1 & -\beta_1 \end{pmatrix}. \tag{C.3}$$

Equation (C.3) is to an extremely high accuracy equivalent to the following equation from which the Nevot–Croce formula directly follows:

$$\boldsymbol{R}_{21} = \frac{1}{t_{12}} \begin{pmatrix} \mathrm{e}^{-(1/2)k_{0z}^2(\beta_1-\beta_2)^2\sigma^2} & r_{21}\mathrm{e}^{-(1/2)k_{0z}^2(\beta_1+\beta_2)^2\sigma^2} \\ r_{21}\mathrm{e}^{-(1/2)k_{0z}^2(\beta_1+\beta_2)^2\sigma^2} & \mathrm{e}^{-(1/2)k_{0z}^2(\beta_1-\beta_2)^2\sigma^2} \end{pmatrix}. \tag{C.4}$$

To verify this equivalence, we have calculated the reflectivity of a Pd boundary for different roughness values. The result is displayed in figure 6.

As it turns out, the roughness matrix developed here leads to practically the same results as the Nevot–Croce formula [31] and, in a slightly different nomenclature, the results obtained by Vidal and Vincent [38]. For high momentum transfer, the reflectivity values calculated from our theory deviate from the Nevot–Croce result in a

[5] We have used the following relations between the Fresnel coefficients: $\mathbf{1} + \boldsymbol{r}_{ij} = \boldsymbol{t}_{ij}$, $\mathbf{1} - \boldsymbol{r}_{ij} = \boldsymbol{t}_{ji}$ and $\boldsymbol{t}_{ji}^{-1}\boldsymbol{t}_{ij} = \boldsymbol{\beta}_j^{-1}\boldsymbol{\beta}_i$.

systematic way and merge into each other asymptotically, independent of the roughness. However, these deviations show up under conditions (low reflectivity, large roughness) that are very likely outside the validity range of both theories anyway.

References

[1] J.P. Hannon, G.T. Trammell, M. Mueller, E. Gerdau, H. Winkler and R. Rüffer, Phys. Rev. Lett. 43 (1979) 636.
[2] J.P. Hannon, N.V. Hung, G.T. Trammell, E. Gerdau, M. Mueller, R. Rüffer and H. Winkler, Phys. Rev. B 32 (1985) 5068 and 5081.
[3] J.P. Hannon, G.T. Trammell, M. Mueller, E. Gerdau, R. Rüffer and H. Winkler, Phys. Rev. B 32 (1985) 6363 and 6374.
[4] M. Grote, R. Röhlsberger, M. Dimer, E. Gerdau, R. Hellmich, R. Hollatz, J. Jäschke, E. Lüken, J. Metge, R. Rüffer, H.D. Rüter, W. Sturhahn, E. Witthoff, M. Harsdorff, W. Pfützner, M. Chambers and J.P. Hannon, Europhys. Lett. 17 (1991) 707.
[5] R. Röhlsberger, E. Gerdau, M. Harsdorff, O. Leupold, E. Lüken, J. Metge, R. Rüffer, W. Sturhahn and E. Witthoff, Europhys. Lett. 18 (1992) 561.
[6] R. Röhlsberger, E. Gerdau, E. Lüken, H.D. Rüter, J. Metge and O. Leupold, Z. Phys. B 92 (1993) 489.
[7] R. Röhlsberger, Dissertation, Universität Hamburg (1994) and Internal Report, DESY, HASYLAB 94-06 (December 1994).
[8] M. Blume and O.C. Kistner, Phys. Rev. 171 (1968) 417.
[9] M. Blume, J. Appl. Phys. 57 (1985) 3615.
[10] J.P. Hannon, G.T. Trammell, M. Blume and D. Gibbs, Phys. Rev. Lett. 61 (1988) 1245; J. Luo, G.T. Trammell and J.P. Hannon, Phys. Rev. Lett. 71 (1993) 287.
[11] D.P. Siddons, M. Hart, Y. Amemiya and J.B. Hastings, Phys. Rev. Lett. 64 (1990) 1967.
[12] T.S. Toellner, E.E. Alp, W. Sturhahn, T.M. Mooney, X. Zhang, M. Ando, Y. Yoda and S. Kikuta, Appl. Phys. Lett. 67 (1995) 1993.
[13] D.P. Siddons, J.B. Hastings, U. Bergmann, F. Sette and M. Krisch, Nucl. Instrum. Methods B 103 (1995) 371.
[14] R. Röhlsberger, E. Gerdau, R. Rüffer, W. Sturhahn, T.S. Toellner, A.I. Chumakov and E.E. Alp, Nucl. Instrum. Methods A 394 (1997) 251.
[15] R.M.A. Azzam and N.M. Bashara, *Ellipsometry and Polarized Light* (Elsevier, Amsterdam, 1987).
[16] S.D. Bader and J.L. Erskine, in: *Ultrathin Magnetic Structures II*, eds. B. Heinrich and J.A.C. Bland (Springer, Berlin, 1994) p. 297.
[17] J.A.C. Bland, in: *Ultrathin Magnetic Structures I*, eds. J.A.C. Bland and B. Heinrich (Springer, Berlin, 1994) p. 305.
[18] In case of perfect single crystals see, e.g., B.W. Batterman and H. Cole, Rev. Modern Phys. 36 (1964) 681.
[19] B. Niesen, M.F. Rosu, A. Mugarza, R. Coehoorn, R.M. Jungblut, F. Rooseboom, A.Q.R. Baron, A.I. Chumakov and R. Rüffer, Phys. Rev. B 58 (1998) 8590.
[20] L. Bottyán, J. Dekoster, L. Deák, A.Q.R. Baron, S. Degroote, R. Moons, D.L. Nagy and G. Langouche, Hyp. Interact. 113 (1998) 295.
[21] J. Bansmann et al., to be published.
[22] J.P. Hannon and G.T. Trammell, Phys. Rev. 169 (1968) 315.
[23] W. Sturhahn and E. Gerdau, Phys. Rev. B 49 (1994) 9285.
[24] A. Krol, C.J. Sher and Y.H. Kao, Phys. Rev. B 38 (1988) 8579.
[25] D.K.G. de Boer, Phys. Rev. B 44 (1991) 498.
[26] Y. Wang, M. Bedzyk and M. Caffrey, Science 258 (1992) 775.

[27] Y.P. Feng, S.K. Sinha, H.W. Deckman, J.B. Hastings and D.P. Siddons, Phys. Rev. Lett. 71 (1993) 537.
[28] S. Lagomarsino, W. Jark, S. DiFonzo, A. Cedola, B. Mueller, P. Engström and C. Riekel, J. Appl. Phys. 79 (1996) 4471.
[29] M. Born and E. Wolf, *Principles of Optics*, 7th ed. (Pergamon, New York, 1978).
[30] S.K. Sinha, private communication.
[31] L. Nevot and P. Croce, Rev. Phys. Appl. 15 (1980) 761.
[32] C.A. Lucas and A.P. Firth, Europhys. Lett. 14 (1991) 343.
[33] M. Tolan, G. König, L. Brügemann, W. Press, F. Brinkop and J.P. Kotthaus, Europhys. Lett. 20 (1992) 223.
[34] R. Röhlsberger, this issue, section IV-1.3.
[35] L. Deák, L. Bottyán, D.L. Nagy and H. Spiering, Phys. Rev. B 53 (1996) 6158.
[36] L. Deák et al., this issue, section VIII-4.
[37] R. Röhlsberger, O. Leupold, J. Metge, H.D. Rüter, W. Sturhahn and E. Gerdau, Hyp. Interact. 92 (1994) 1107.
[38] B. Vidal and P. Vincent, Appl. Opt. 23 (1984) 1794.